Received March 24, 2021, accepted April 11, 2021, date of publication April 22, 2021, date of current version May 3, 2021.

Digital Object Identifier 10.1109/ACCESS.2021.3074922

Improving the Performance of SDM-EON Through Demand Prioritization: A Comprehensive Analysis

PATRICIA MORALES[1], ASTRID LOZADA[1], DANILO BÓRQUEZ-PAREDES[2], RICARDO OLIVARES[1], GABRIEL SAAVEDRA[3], (Member, IEEE), ARIEL LEIVA[4], (Member, IEEE), ALEJANDRA BEGHELLI[5], AND NICOLÁS JARA[1], (Member, IEEE)

[1]Department of Electronic Engineering, Universidad Técnica Federico Santa María, Valparaíso 2390123, Chile
[2]Faculty of Engineering and Science, Universidad Adolfo Ibáñez, Santiago 7941169, Chile
[3]Electrical Engineering Department, Universidad de Concepción, Concepción 4070409, Chile
[4]School of Electrical Engineering, Pontificia Universidad Católica de Valparaíso, Valparaíso 2362804, Chile
[5]Department of Electronic and Electrical Engineering, University College London, London WC1E 7JE, U.K.

Corresponding author: Patricia Morales (patricia.morales@sansano.usm.cl)

This work supported in part by under Grant DI-PUCV 039.437, in part by under Grant USM PI LII_2020_74, in part by USM PIIC 021/2021, in part by under Grant Agencia Nacional de Investigación y Desarrollo (ANID) 21200588, and in part by ANID FONDECYT Iniciación under Grant 11201024 and Grant 11190710.

ABSTRACT This paper studies the impact of demand-prioritization on Space-Division Multiplexing Elastic Optical Networks (SDM-EON). For this purpose, we solve the static Routing, Modulation Level, Spatial Mode, and Spectrum Assignment (RMLSSA) problem using 34 different explainable demand-prioritization strategies. Although previous works have applied heuristics or meta-heuristics to perform demand-prioritization, they have not focused on identifying the best prioritization strategies, their inner operation, and the implications behind their good performance by thorough profiling and impact analysis. We focus on a comprehensive analysis identifying the best explainable strategies to sort network demands in SDM-EON, considering the physical-layer impairments found in optical communications. Also, we show that simply using the common shortest path routing might lead to higher resource requirements. Extensive simulation results show that up to 8.33 % capacity savings can be achieved on average by balanced routing, up to a 16.69 % capacity savings can be achieved using the best performing demand-prioritization strategy compared to the worst-performing ones, the most used demand-prioritization strategy in the literature (serving demands with higher bandwidth requirements first) is not the best-performing one but the one sorting based on the path lengths, and using double-criteria strategies to break ties is key for a good performance. These results are relevant showing that a good combination of routing and demand-prioritization heuristics impact significantly on network performance. Additionally, they increase the understanding about the inner workings of good heuristics, a valuable knowledge when network settings forbid using more computationally complex approaches.

INDEX TERMS Elastic optical networks, space-division multiplexing, resource assignment, network capacity, physical-layer impairments.

I. INTRODUCTION

The overall Internet traffic continues to grow due to the ever-increasing popularity of established and emerging network services and applications [1]. Nowadays, such traffic growth can only be supported by the current installed optical network infrastructure. However, several researchers have alerted about the imminent capacity exhaustion of core optical networks, a situation known as ''capacity crunch'' [2].

Among the several possible solutions to avoid capacity exhaustion in core networks, two main courses of action can be distinguished:

The associate editor coordinating the review of this manuscript and approving it for publication was Tianhua Xu.

A. EFFICIENT MANAGEMENT OF NETWORK RESOURCES

Elastic Optical Networks (EON) is a new spectrum usage scheme that increases the efficiency of spectrum utilization [3]–[5]. Such higher efficiency is achieved by dividing the spectrum into small sections with fixed bandwidth, called frequency slot units (FSUs). FSUs can be grouped to satisfy the bandwidth required by each demand adaptively. State-of-the-art experimental results have shown the feasibility of spectral widths of 12.5 GHz and 6.25 GHz [6].

B. CAPACITY INCREASE

Using already deployed fibers, their capacity can be increased by extending the operation band from the usual C-band (between 1530 nm and 1565 nm) to the L, S, E, and O bands [7], [8]. Alternatively, current single-mode fibers can be replaced by novel fibers that support Space Division Multiplexing (SDM). The most straightforward SDM approach is based on the transmission of information over multiple traditional single-mode fiber (SMF) pairs, known as SMF bundle (SMF-B) [1]. However, newly emerging fiber types are designed explicitly for SDM, comprising multiple fiber cores (i.e., multicore fibers - MCF), supporting several propagation modes over one fiber core (i.e., multimode fibers - MMF), or a combination of both as in few mode-multicore fibers (FM-MCF) [1]. MMF is made of a single fiber core of enlarged diameter and a modified refractive index profile that enables parallel transmission of several co-propagating spatial modes [9]–[11]. In MCF, multiple cores are placed within a single fiber cladding, with each core behaving like a separate fiber cable [1], [12].

Both EON and SDM technologies offer complementary solutions to confront the ''capacity crunch'' problem in optical communications [13]. Therefore, research on the potential benefits of their joint operation has already started [1], [10]. However, they also introduce a wide range of new challenges in terms of equipment such as fiber, multiplexers/demultiplexers, amplifiers, and ROADMs able to work over the new spatial dimensions [14]. Also, the multitude of spatial modes introduces new physical layer impairments that need to be taken into account when modeling the quality of transmission in SDM fiber links [15]. From a resource allocation point of view, the main challenge in establishing optical connections is the efficient usage of spectrum resources despite the detrimental effect of the spectrum continuity and contiguity constraints and the spatial-mode parallelism [1], [5].

Such efficient spectrum usage must be enabled by a good resource allocation algorithm to establish optical connections. In a multi-spectrally and spatially elastic optical network, this algorithm is known as the Routing, Modulation Level, Spatial mode, and Spectrum Assignment (RMLSSA) algorithm [16]–[19]. An RMLSSA algorithm is in charge of finding a path - an optical connection between two network nodes - to each network demand (routing), a modulation format that achieves a good trade-off between spectrum usage and optical reach (modulation level) [20], a specific fiber core (spatial mode) and a set of contiguous and continuous FSUs (spectrum) on the selected route and core.

For transparent optical communications, RMLSSA algorithms must comply with the following constraints: first, each FSU can host only one demand; second, the set of FSUs assigned to a given demand must be maintained along the entire origin-destination route, known as the *"continuity constraint"*; also, if the demand's bandwidth requirement must be satisfied allocating more than one FSU, the assigned FSUs must be consecutive in the spectrum, known as the *"contiguity constraint"* [5]. Finally, depending on the SDM technology used and the distance between cores, crosstalk could prevent the simultaneous use of the same FSUs in adjacent cores.

In a static scenario, demands are known before the network starts operating, and thus, the establishment of optical connections is done offline. That is, a traffic matrix with the requested transmission data rates of all connection demands is given as input data for the resource allocation process [13]. In this type of network, optical paths are assigned quasi-permanently, that is, connections remain established on time scales from days to years [21], [22], as is the case in today's optical WDM networks. Although dynamic operation might bring further efficiency in terms of resource usage, previous work in the context of WDM networks has shown that this is not the case due to the wavelength continuity constraint [23]. Given the contiguity and continuity constraints imposed by EONs, the eventual advantages of dynamic operation in EONs might not compensate for the increased complexity of devices and the control plane. In fact, the literature discussion points first to evolution from current static WDM optical networks towards static EONs (for efficient usage of the installed spectrum), and then, incorporating SDM techniques to increase the network capacity [24], [25]. Thus, as in [13], in this paper, we solve the static RMLSSA problem.

The efficiency of resource allocation algorithms for static operation networks can be measured in two ways: by evaluating the maximum amount of demands that can be served with a given capacity or by quantifying the minimum network capacity required to accommodate a given demand [1], [26], [27]. In this work, we use the former approach. Capacity minimization as the main objective of a static RMLSSA allocation algorithm can be optimally solved by using optimization techniques such as integer linear programming (ILP) or mixed-integer linear programming (MILP) models [28]–[31]. However, the RMLSSA problem is known to be NP-complete [1], [32]. As a result, its computational complexity makes an optimal RMLSSA solution's execution time prohibitively high, even for small networks [1], [33]. For example, in [13], it was shown that the ILP solver running time could be as high as 72 hours for six-node networks.

On the contrary, heuristic (and meta-heuristic) methods do not guarantee optimal solutions, but scale to higher order networks with relatively fast execution times. For example, in [13], four different heuristic approaches executed in

the same six-node networks in less than a second. In [34] and [35], the authors compare the behavior of an optimal ILP RMLSA algorithm minimizing the spectrum usage, a heuristic algorithm serving connections one by one using 2 different order criteria, and a simulated annealing meta-heuristic approach. Results indicate that sequential heuristic combined with an appropriate ordering can give near-optimal solutions in low running times. In addition, according to [1], although meta-heuristics are widely used to solve resource allocation problems in SDM (such as [18], [36]–[38]), heuristics are extensively used too ([16]–[18], [32], [36], [37], [39]–[42]). Heuristic solutions for the RMLSSA problem are usually solved in sequential stages [5], [31]. First, a route is assigned (typically, the shortest path); then, a suitable modulation format is chosen (usually, the one that decreases the number of FSUs required given length of the route); and finally the FSUs and cores on each link are assigned [43].

As a consequence of the sequential solving of the RMLSSA problem and the contiguity and continuity constraints, it is usual to find unallocated FSUs surrounded by allocated ones. This situation, known as fragmentation, is undesirable because it might prevent attending additional demands due to inefficient capacity usage. Therefore, a common goal of RMLSSA solutions is to decrease fragmentation to maximize capacity utilization [29], [30].

Several papers, [1], [13], [16], [18], [32], [34], [35], [41], [44]–[46], show that the order in which demands are served impacts the network fragmentation and, thus, the network capacity requirements. However, they carry out partial studies where only a handful of prioritization strategies are researched. Having a strategy that defines what demand will be allocated resources first (demand-sorting strategy) is relevant when the network operates statically or when a defragmentation operation needs to be performed in a dynamic environment [47]–[51]. In the latter case, currently established connections are re-allocated to increase the available capacity. In most papers that use a demand-sorting strategy, demands are sorted by their spectrum requirements [1], [13], [16], [18], [32], [44], while others sort demands based on their path lengths (in km or number of links) [1], [41], [45]. Despite the importance of the demand-sorting strategy on the network capacity requirements, no previous work has carried out a comprehensive comparative study of the impact of different demand-sorting strategies on network performance. Common demand-sorting strategies found in the literature serve first the demands with the highest FSUs requirements, without contrasting its performance to other sorting schemes. Additionally, most previous works have not considered the physical-layer impairments (PLI) on the analysis. In such an ideal network environment, the FSU requirements and path lengths are not related. However, considering the PLI on the equation introduces a maximum optical reach for each data transmission, which might restrict the modulation formats available for each demand to the ones demanding more FSUs to transmit. This situation leads to a correlation between path lengths and bandwidth demands. Such a correlation has not been considered on the way demands are prioritized to be allocated resources.

In this work, we study for the first time 34 different explainable demand-sorting strategies and evaluate their impact on the network performance for SDM-EON, considering the PLI found in SDM-EON communications. We analyze different sorting strategies in terms of network fragmentation, network capacity requirement, and distribution of the modulation formats in the fiber cores. In this sense, we profile the strategies used identifying the best ones according to the topology. Such knowledge is of interest to network operators, not only because the performance of the network is improved by efficient usage of network capacity but also because a further understanding of the inner working of heuristics is useful when the network setting forbids the use of more computationally complex approaches.

The remainder of this paper is as follows: Section II describes the RMLSSA strategy used in this work. Section III presents the demand-sorting strategies used to test the proposed RMLSSA algorithm. Section IV discusses the numerical results. Finally, conclusions and remarks are drawn in Section V.

II. RMLSSA AND DEMAND-SORTING STRATEGIES

In this section, the physical layer impairment model used to determine the number of FSU's allocated to each demand is described. Then, the RMLSSA algorithm used to allocate network resources is presented. Finally, the 34 demand-sorting strategies studied in this paper are detailed.

A. PHYSICAL LAYER IMPAIRMENTS MODEL

The quality of transmission (QoT) of optical signals is degraded by different phenomena occurring during the modulation, propagation, and detection processes. In particular, to solve the RMLSSA problem, we consider the impact that the amplified spontaneous emission (ASE) noise and non-linear interference noise have on the QoT. The accumulation of noise during propagation determines the maximum optical reach that a signal can have for a given modulation level and bit error rate (BER) combination. Complex modulation formats, with a high number of bits per symbol, increase the transmission sensitivity to degradation. Thus, the transmission reach is shorter for higher modulation levels compared to simpler formats [13]. To consider this *route length - modulation level* trade-off, the most common approach is to associate any modulation format available at the transponder to its maximum transmission reach for a given BER value [1], [29]. This is also the approach used in this work.

The modulation formats considered in this study are binary phase-shift keying (BPSK), quadrature phase-shift keying (QPSK), and Λ-quadrature amplitude modulation (Λ-QAM), where Λ takes the values 8, 16, 32, and 64, as shown in the first column of Table 1. The second column in the table shows the maximum achievable reach (MAR) - assuming single-polarization - as a function of the modulation format

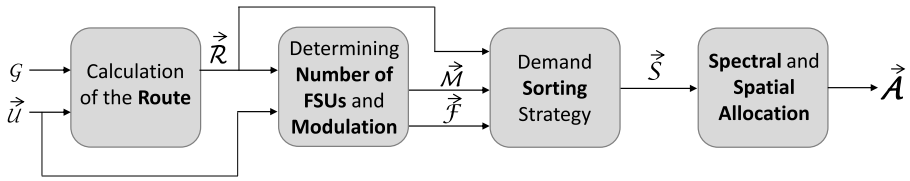

FIGURE 1. Schematic of the RMLSSA algorithm: input data, intermediate steps and output data.

TABLE 1. Maximum achievable reach (MAR) per modulation format and FSU requirements per bit-rate and modulation format pair, for a BER value equal to 10^{-6}.

Modulation	MAR [km]	Bitrates [Gbps]				
		10	40	100	400	1000
BPSK	5520	1	4	8	32	80
QPSK	2720	1	2	4	16	40
8-QAM	1360	1	2	3	11	27
16-QAM	560	1	1	2	8	20
32-QAM	240	1	1	2	7	16
64-QAM	80	1	1	2	6	14

available at the transponders. The optical reach values were obtained using the GN model [52] to estimate the received signal-to-noise ratio (SNR) degraded by ASE noise and non-linear interference noise. The SNR calculated based on the GN model is compared with the minimum SNR value required to guarantee a BER threshold for each available modulation format. This procedure allows us to determine the maximum number of spans that can be transmitted at optimum launch power. Thus, the MAR for each modulation format shown in Table 1 corresponds to the maximum length, in kilometers (a multiple of the number of 100-km spans), that an optical signal can travel without exceeding a BER of 10^{-6}. The MAR was calculated considering a worst case scenario, fully-loaded C-band with 320 FSU slots occupied by signal with a bandwidth equal to one FSU. For more details about the optical reach calculation, the reader is referred to [20], Section III. In this work crosstalk between spatial modes was not considered. That is, the reach was estimated for a SDM channel formed by MCF with reduced crosstalk, e.g. trench-assisted or increased core-to-core distance, or a SMF-B. Remark that crosstalk reduces the transmission reach in a SDM channel, however, this has a limited impact on the strategies to sort the demands studied herein. The remaining columns in Table 1 show the required number of FSUs necessary to form a super-channel with different bit rates for each modulation format under consideration.

B. RMLSSA ALGORITHM

Figure 1 shows an schematic of the RMLSSA solver used in this study, which employs well-known spectrum assignment and routing algorithms, but introduces a demand-sorting step prior to spectrum allocation (step 3 "Demand sorting strategy" in Figure 1).

In our RMLSSA solver the inputs are:

- graph $\mathcal{G} = (\mathcal{N}, \mathcal{E}, \mathcal{K})$, where $\mathcal{N}$ is the set of nodes in the network, $\mathcal{E}$ the set of unidirectional links - each with a capacity expressed in number of FSUs - and $\mathcal{K}$ the set of cores in all the network links (represents the number of cores to assign all demands), with cardinality N, E y K respectively.
- the demand vector $\vec{\mathcal{U}}$, with elements in the form $\langle s_u, d_u, b_u \rangle$, where s_u is the source node, d_u the destination node, and b_u the bit rate associated to demand u.

The first step computes a route for each demand in $\vec{\mathcal{U}}$, storing them on the vector $\vec{\mathcal{R}}$. Each element in $\vec{\mathcal{R}}$ has the form $\langle r_u, \ell_u \rangle$ where r_u and ℓ_u represent the route and its length (in kilometers), respectively, for demand u. These routes are fixed and can be computed by any algorithm available in the literature [53]–[56]. In algorithmic form, we symbolically write $\vec{\mathcal{R}} := \text{Routing}(\mathcal{G}, \vec{\mathcal{U}})$.

The second step uses the route length information from $\vec{\mathcal{R}}$ and the required bit rate from $\vec{\mathcal{U}}$ to determine - using Table 1 - the most efficient modulation format and the number of FSUs needed. In Table 1, the modulation formats are sorted in increasing order of spectral efficiency. Therefore, the most efficient modulation format with a MAR value equal to or higher than the route length is selected. As a result, the vectors $\vec{\mathcal{M}}$ and $\vec{\mathcal{F}}$ are generated. The vectors $\vec{\mathcal{M}}$ and $\vec{\mathcal{F}}$ are comprised of m_u the modulation format and f_u the number of FSUs required for each demand, respectively. In algorithmic form, we symbolically write $\{\vec{\mathcal{M}}, \vec{\mathcal{F}}\} := \text{ModFSU}(\mathcal{R}, \mathcal{U})$.

Next, the demands in $\vec{\mathcal{U}}$ are sorted according to one or more criteria. Different strategies consider different criteria to perform the sorting. Depending on the strategy used, the information contained in the vectors $\vec{\mathcal{R}}$, $\vec{\mathcal{M}}$ and $\vec{\mathcal{F}}$ might be used to sort the demands. As a result, the vector $\vec{\mathcal{S}} = \text{sort}(\vec{\mathcal{R}}, \vec{\mathcal{M}}, \vec{\mathcal{F}})$ is generated, which now contains the ordered demands. In algorithmic form, we symbolically write $\vec{\mathcal{S}} := \text{Sorting}(\vec{\mathcal{R}}, \vec{\mathcal{M}}, \vec{\mathcal{F}})$.

Finally, for each element in $\vec{\mathcal{S}}$, the First Fit SSA procedure is executed to allocate FSUs and one core along the route. The FSU allocation procedure must comply with spectrum continuity and contiguity constraints [5], [12]. In SDM technologies an additional core continuity constraint might also be taken into account. In that case, only one core needs to be allocated. The core continuity constraint has the potential to

simplify the node architecture [57]. In this work, we analyze the network performance considering that the core continuity constraint is in place.

The output of the SSA is the allocation vector $\vec{\mathcal{A}}$. Each element in $\vec{\mathcal{A}}$ has the form $\langle r_u, i_u, f_u, \vec{\mathcal{V}} \rangle$ where r_u is the route for demand u, i_u is the identification of the first FSU where the demand must be allocated in every link, f_u is the number of FSUs required by the demand u, and $\vec{\mathcal{V}}$ is the core vector. Each element in $\vec{\mathcal{V}}$ corresponds to the core where each route link of the demand was assigned. Under the core continuity constraint, the core vector collapses to a single element.

Algorithm 1 shows the pseudo-code of the proposed RMLSSA algorithm, including the intermediate steps explained above.

Lines 2 **to 3** perform the calculation of all demand paths $\vec{\mathcal{R}}$, their modulation formats $\vec{\mathcal{M}}$, and their corresponding FSU requirements $\vec{\mathcal{F}}$.

In **line 4**, the demand-sorting procedure is executed. Remark that the sorting function will output different results depending on the sorting criteria, as explained in Subsection II-C. This procedure returns the vector $\vec{\mathcal{S}}$, which contains the same set of demands in the vector $\vec{\mathcal{U}}$, but now ordered according to some criteria.

In **line 5** the assignment vector $\vec{\mathcal{A}}$ is initialized. This vector corresponds to the algorithm's output and stores all the information of each demand: route, FSUs, and core allocation.

In **lines 6 to 17**, an iterative procedure that searches for a subset of FSUs in a specific core for each demand u is executed (the so-called SSA algorithm). The iterative procedure ends when all demands have been assigned resources (**line 7**). We use a version of the First-Fit algorithm, modified for the SDM-EON architecture. Thus, we start checking the availability of the first FSU (i_u equal to 0, **line 8**) on the first core (k equal to 1, for loop in **line 9**). Let i_{uk}^{max} be the maximum number of FSUs in link $e \in r_u$ on the k-th core. From **lines 10 to 17** we search for a number of f_u available FSUs on the path r_u on the k-th core. The set of f_u FSUs must comply with the continuity and contiguity constraints. Therefore, the search proceeds from the first FSU to the $i_{uk}^{max} - f_u - 1$ slot (**lines 10 and 16**). Once a set of contiguous f_u FSUs is found in every link of the route in the k-th core (**line 11**), the set of FSUs is assigned to the demand u (**line 12**), the vector $\vec{\mathcal{A}}$ is updated with the corresponding information about the route, FSUs and core for demand u $\langle r_u, i_u, f_u, \vec{\mathcal{V}} \rangle$ (**line 13**).

By repeating the steps explained above for each demand in $\vec{\mathcal{S}}$ (**lines 6 to 17**), we update the output vector $\vec{\mathcal{A}}$ (**line 18**).

C. DEMAND-SORTING STRATEGIES

As previously mentioned in section II-B, we add an explicit step in the RMLSSA algorithm where the demands are sorted prior to space and spectrum assignment procedure (SSA). Sorting demands before performing the spectrum and space allocation might significantly decrease network fragmentation, and thus, achieve significant network capacity savings. We identified 34 demand-sorting strategies that use different sorting criteria based on the number of FSUs requested by the demand, the length of the path, and network usage. We classified these strategies into 6 groups, as shown in Table 2. They are as follows:

- *Group 1:* Demands are randomly sorted using a uniform distribution (Strategy 1). This group represents the case where demands are not sorted according to any specific criteria.
- *Group 2:* Demands are sorted using a single criterion. Strategies **2, 4, 6** sort demands in descending order of number of FSUs, route distance (in km), and route number of links (hop count). Strategies **3, 5, 7** sort demands in ascending order of number of FSUs, route distance (in km), and route number of links.
- *Group 3:* Demands are sorted using either descending or ascending double criteria. Even-numbered strategies (**8-18**) use descending criteria while odd-numbered ones (**9-19**) use ascending criteria. The first criterion sorts the demands and the second breaks ties. For example, Strategy **8** sorts demands in descending order of number of route links. If two routes have the same number of links, then they are sorted in descending order of number of FSUs.
- *Group 4:* Demands are sorted using mixed double criteria: one criterion in descending order and the other in ascending order. As with the previous group, Strategies **20-31** use the first criterion to sort the demands and the second to break ties. For example, Strategy **20** sorts demands in descending order of number of route links. If two routes have the same number of links, then they are sorted in ascending order of number of FSUs.
- *Group 5:* Strategy **32** sorts demands in descending order of link utilization (number of routes using a link). All demands belonging to the same link are then sorted in descending order of the number of FSUs times the number of links in the route.
- *Group 6:* Mixed multiplicative criteria. Strategies **33** and **34** sort demands in descending and ascending order of number of FSUs times the number of links, respectively.

III. SIMULATION SCENARIOS

The performance evaluation of the RMLSSA algorithm was carried out using an event-discrete simulator written in Python. Different simulation scenarios defined by 6 different network topologies and the 34 demand-sorting strategies described in the previous section were analyzed (204 scenarios). Next, we discuss the characteristics of the networks used for the simulations, the traffic generation method, and the performance metrics used.

A. NETWORK TOPOLOGIES

The main network characteristics assumed for the topologies used for this study are summarized in Table 3. The number of cores is not limited to any specific value, as the aim of this study is to quantify the network capacity requirements.

Algorithm 1 RMLSSA Proposal

procedure RMLSSA($\mathcal{G}, \vec{\mathcal{U}}$)
  $\vec{\mathcal{R}} :=$ Routing($\mathcal{G}, \vec{\mathcal{U}}$);
  $\{\vec{\mathcal{M}}, \vec{\mathcal{F}}\} :=$ ModFSU($\vec{\mathcal{R}}, \vec{\mathcal{U}}$);
  $\vec{\mathcal{S}} :=$ Sorting($\vec{\mathcal{R}}, \vec{\mathcal{M}}, \vec{\mathcal{F}}$);
  $\vec{\mathcal{A}} = \phi$;
  for each demand in $\vec{\mathcal{S}}$ **do**
    while demand not assigned **do**
      $i_u := 0$;
      for all $k \in \mathcal{K}$ **do**
        while $i_u \leq i_{uk}^{max} - f_u - 1$ **do**
          if FSUs from i_u to $i_u + f_u - 1$ are free in k-th core of r_u **then**
            Assign the slots to demands u in k-th core of r_u;
            Add demands u and its chosen core and slots in $\vec{\mathcal{A}}$
            Break;
          else
            $i_u := i_u + 1$;
        $i_u := 0$;
  return $\vec{\mathcal{A}}$

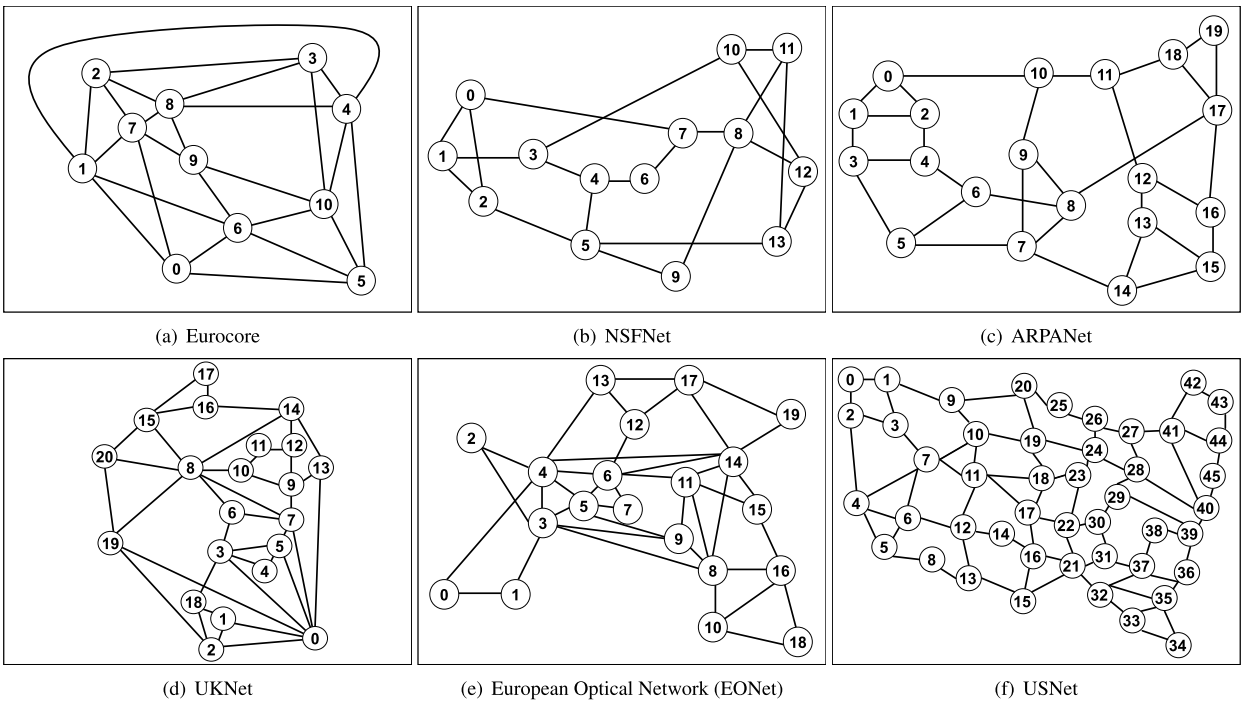

(a) Eurocore (b) NSFNet (c) ARPANet

(d) UKNet (e) European Optical Network (EONet) (f) USNet

FIGURE 2. Network topologies.

To evaluate the behavior of the proposed algorithm in different network scenarios, the 6 real network topologies shown in Figure 2 were used.

The network capacity of each topology is determined by the C-band frequency spectrum. Assuming an FSU spectral width of 12.5 GHz, this leads to a total of 320 FSUs per link in every core. The number of fiber cores used on the multicore fibers will not be fixed beforehand, so we can evaluate the maximum number of cores needed to allocate all transmission requests.

B. TRAFFIC GENERATION

One traffic demand per node pair is generated, yielding a total of $|\mathcal{N}| \cdot (|\mathcal{N}| - 1)$ demands. However, if a demand has a shortest path longer than the maximum reach allowed by the less efficient modulation format (5220 km, please see Table 1), it is not included in the input set $\vec{\mathcal{U}}$. The bit rate of each traffic demand is generated randomly from the set {10 Gbps, 40 Gbps, 100 Gbps, 400 Gbps, and 1000 Gbps}. To make the different simulation scenarios comparable, we use the same seeds in all of them, so the same set of demand requests is

TABLE 2. Demand-sorting strategies.

Group 1	
1-Unsorted	
Group 2	
2-FSU ↓	**3**-FSU ↑
4-Distance ↓	**5**-Distance ↑
6-Link ↓	**7**-Link ↑
Group 3	
8-Link ↓ FSU ↓	**9**-Link ↑ FSU ↑
10-FSU ↓ Link ↓	**11**-FSU ↑ Link ↑
12- Link ↓ Distance ↓	**13**-Link ↑ Distance ↑
14-FSU ↓ Distance ↓	**15**-FSU ↑ Distance ↑
16-Distance ↓ Link ↓	**17**-Distance ↑ Link ↑
18-Distance ↓ FSU ↓	**19**-Distance ↑ FSU ↑
Group 4	
20-Link ↓ FSU ↑	**21**-Link ↑ FSU ↓
22-FSU ↓ Link ↑	**23**-FSU ↑ Link ↓
24-Link ↓ Distance ↑	**25**-Link ↑ Distance ↓
26-FSU ↓ Distance ↑	**27**-FSU ↑ Distance ↓
28-Distance ↓ Link ↑	**29**-Distance ↑ Link ↓
30-Distance ↓ FSU ↑	**31**-Distance ↑ FSU ↓
Group 5	
32- + Link ↓ (FSU x Link) ↓	
Group 6	
33-(FSU x Link) ↓	**34**-(FSU x Link) ↑

TABLE 3. Network characteristics.

Parameter	Value
Capacity per link	320 slots
Number of cores	Unlimited
Bitrates	10, 40, 100, 400, 1000 Gbps
Modulation formats	BPSK, QPSK, 8-QAM, 16-QAM, 32-QAM, 64-QAM
FSUs and MAR	Table 1

generated. For each simulation scenario, a total of 100 simulation runs are executed.

C. PERFORMANCE METRICS

To evaluate the performance of the different demand-sorting strategies in all the network topologies we used performance metrics related to: 1) the network capacity required to accommodate all demands, 2) spectrum fragmentation and, 3) spectrum usage. These are explained in the following.

1) EFFECTIVE NETWORK CAPACITY REQUIREMENT

We store the capacity of all network links in vector $\vec{C}$. The element $c_e \in \vec{C}$ is the total capacity of link e in number of FSUs. The value of c_e is calculated as $c_e = \sum_{\forall \mathcal{K}} c_{e,k}$, where $c_{e,k}$ is the total amount of FSU on the k-th core of link e.

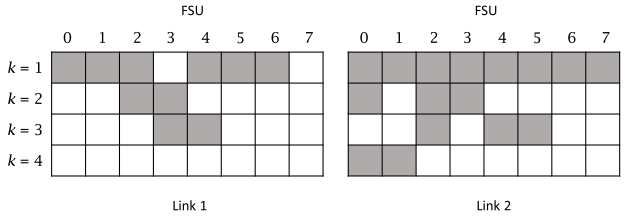

FIGURE 3. Example of space and spectrum assignment (SSA) on a two links arbitrary network.

Besides, let us define the effective link capacity $\hat{c}_e$ as the capacity used on link e, including fragmented slots. To compute the value of $\hat{c}_e$, first, the last fiber core used in link e, denoted by $\hat{k}$, must be identified. Then, the number of slots between the first slot of core $\hat{k}$ (FSU = 0) and the last slot allocated to any demand in core $\hat{k}$ must be recorded. This number is the effective core capacity of the last core $\hat{k}$, denoted by $\hat{c}_{e,\hat{k}}$. Then, we compute $\hat{c}_e$ for each link as follows:

$$\hat{c}_e = \sum_{k=1}^{\hat{k}-1} (c_k) + \hat{c}_{e,\hat{k}}, \tag{1}$$

Figure 3 exemplifies the calculation of $\hat{c}_e$. In the figure, the slot usage of two 8-slot 4-core network links is represented by means of matrices. Each row represents a core and each column an FSU. If an FSU is assigned to a demand, its corresponding square is filled with gray.

In this example, the last core used on link 1 is $\hat{k} = 3$, and thus, $\hat{c}_{1,\hat{3}} = 5$. Consequently, the effective link capacity c_e is equal to $8 + 8 + 5 = 21$. Similarly, on link 2 $\hat{k}$ is equal to 4, $\hat{c}_{2,\hat{4}} = 2$, and $c_2 = 26$.

The sum of the effective link capacities across all network links determines the effective network capacity requirement ($\hat{C}_{net}$), commonly used to evaluate RSA algorithms [29], [58]. That is:

$$\hat{C}_{net} = \sum_{e \in \mathcal{E}} \hat{c}_e. \tag{2}$$

Back to the example shown in Figure 3, if links 1 and 2 were all the network links, then the effective network capacity would be equal to 47. Remark that, any non-used capacity included in the effective link capacity is considered as fragmentation (e.g., FSU 3 in core 1 on link 1 or FSU 6, core 3 on link 2), as explained next.

2) FRAGMENTATION

As mentioned in Section I, fragmented FSUs on the network links should be avoided because the continuity and contiguity constraints make it difficult to use them to allocate demands [59]. Thus, they usually constitute a waste of network resources.

Network fragmentation in a static scenario [60] is defined as the number of unused FSUs within the network effective capacity. In SDM architectures we can recognize two types

of fragmentation: spectral fragmentation (**SpecF**) and spatial fragmentation (**SpatF**) [1], [13].

Spectral fragmentation is the number of unused FSUs surrounded by allocated FSUs. For example, in Figure 3 the SpecF of link 1 is equal to 6 FSUs (core 1, FSUs 3; core 2, FSUs 0,1; core 3, FSUs 0-2) and the total network SpecF (assuming a network made of these 2 links) is equal to 10 FSUs.

Spatial fragmentation is the number of unused FSUs located in the last part of the fiber cores $0, 1, \ldots \hat{k} - 1$. Such fragmentation is mainly due to the splitting of the total capacity into several network cores. For instance, in Figure 3, the value of SpatF in link 1 is equal to 5 FSUs (core 1, FSU 7; core 2, FSUs 4-7) and the total SpatF is equal to 11 FSUs. These FSUs are - with a high probability- not useful to serve more demands since demands would usually require a number of FSUs larger than those available in that part of the core.

We consider that the last fiber core used in each link does not contribute to the spatial fragmentation, since those slots may still be enough to attend new demands.

The total fragmentation experienced by the overall network is due to the contribution of the spectral and spatial fragmentation [1], [13]. We called this parameter Total Frag, evaluated using Eq. (3).

$$\text{Total Frag} = \text{SpecF} + \text{SpatF}. \tag{3}$$

In the example of Figure 3 the total fragmentation given by Eq. (3) is Total Frag $= 10 + 11 = 21$. In this sense, we define the percentage of fragmentation - Total Frag (%) - as the proportion of the effective capacity affected by fragmentation.

Consequently, we compute this metric as follows (Eq (4)):

$$\text{Total Frag (\%)} = 100 \cdot \frac{\text{Total Frag}}{\hat{C}_{net}}. \tag{4}$$

In the example of Figure 3, Total Frag (%) is computed as $100 \cdot (\frac{21}{47}) = 44.68$ %. The lower this value the better the performance of the allocation algorithm.

3) PERCENTAGE OF SPECTRUM USAGE

Finally, to allow comparison across different topologies, we define the percentage of used FSUs - Total Used FSUs (%) - as the proportion of the effective capacity affected by used FSUs. Consequently, we compute this metric as follows (Eq (5)):

$$\text{Total Used FSUs (\%)} = 100 \cdot \frac{\text{Used FSUs}}{\hat{C}_{net}}. \tag{5}$$

In the example of Figure 3, Total Used FSUs (%) is computed as $100 \cdot \frac{26}{47} = 55.32$ %.

Notice that although the number of used FSUs (Used FSUs) is the same for all strategies (since the same traffic demand is served), the number of used FSUs normalized to the effective capacity does change. As a result, the closer this value is to 100 %, the better the performance of the algorithm.

TABLE 4. Average value of total used FSUs(%) for the Shortest Path (SPR) and Baroni (BR) routing algorithms for the 34 demand sorting strategies on all network topologies studied here.

Topology	**SPR** (avg %)	**BR** (avg %)	Difference
Eurocore	79.38	83.64	4.26
NSFNet	60.98	66.04	5.06
ARPANet	46.46	50.66	4.2
UKNet	49.19	61.97	12.78
EONet	54.19	62.95	8.76
USNet	39.61	54.58	14.97

IV. NUMERICAL RESULTS

In this section, we report on the simulation results obtained by executing the RMLSSA algorithm on the topologies shown in Figure 2 considering the 34 different demand-sorting strategies shown in Table 2.

We analyzed two main scenarios: one scenario where the bit rates defined in Table 3 are randomly assigned for each connection request and a worst-case scenario, where all demands request 1000 Gbps. Due to the lack of space, we report on the most critical scenario (1000 Gbps per demand). Notwithstanding, both scenarios obtained the same relative results.

A. IMPACT OF THE ROUTING ALGORITHM

In this section, we executed the RMLSSA algorithm (for the 34 different demand-sorting strategies) using 2 routing algorithms found in the literature: Shortest Path Routing (SPR) and Baroni's Routing (BR). In the former case, Dijkstra's algorithm was executed using the length of the links (in km) to find the shortest route. In the latter, the heuristic proposed in [61] is used. This method seeks to balance the number of routes passing through each link iterating among all possible shortest paths and possible paths with one extra link found for each demand.

Figure 4 shows the percentage of Total Used FSUs (%), corresponding to the value of all allocated FSUs normalized to the effective network capacity, computed by the RMLSSA method explained in section II using the SPR and BR routing strategies, for the 34 demand-sorting strategies analyzed in this paper for the Eurocore, NSFNet and ARPANet network topologies. Similar results were obtained for the UKNet, EONet and, USNet topologies, but we omitted them in the figure to improve image clarity.

As seen in Figure 4, balancing the demands across the network links (BR) achieves better efficiency in the use of the spectrum compared to simply using the shortest path (SPR), irrespective of the demand-sorting strategy used. Table 4 shows the average value of Total Used FSU(%) achieved by the SPR and BR routing techniques for the 34 demand sorting strategies for all topologies. Remark that the highest difference in percentage of Used FSUs between the SPR and BR routing strategies occurs in the USNet network topology, where BR achieves 14.97 % more Total Used FSUs. On the

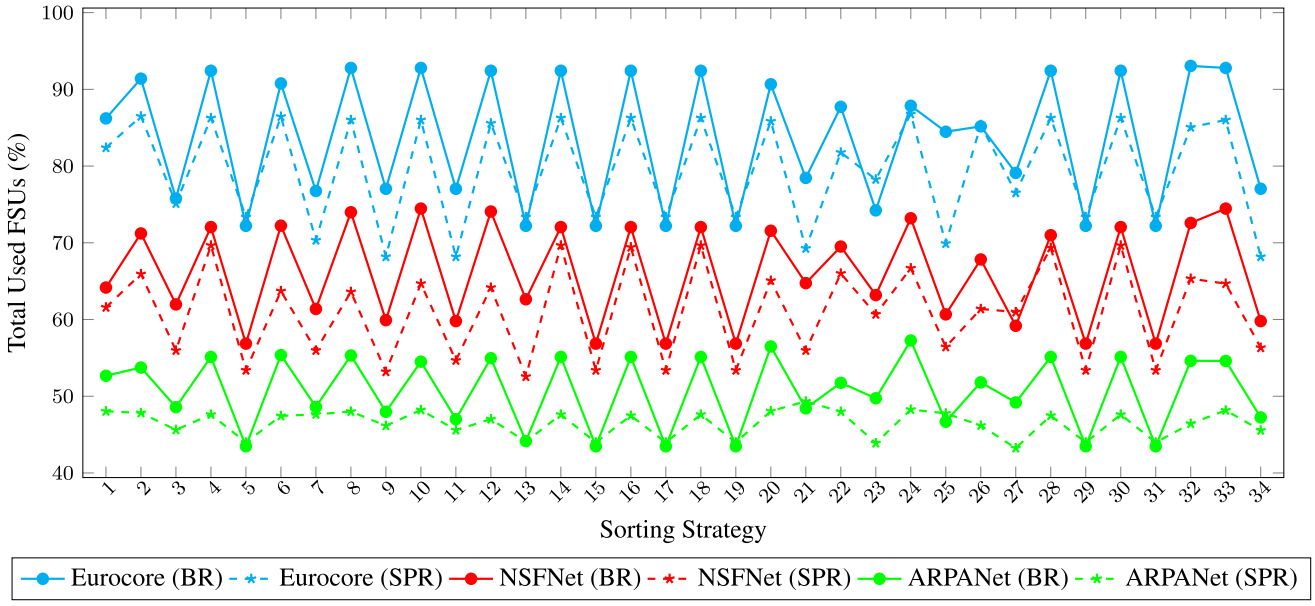

FIGURE 4. Percentage of Used FSUs -Total Used FSUs (%)- obtained by the RMLSSA method using Baroni (BR) and Shortest Path (SPR) routing methods and the 34 demand sorting strategies for Eurocore, NSFNet and ARPANet.

other side, the smallest gap is obtained by the ARPANet network topology with a 4.20 %. We can see that, in general, the higher the order of the network, the more significant the savings achieved (in terms of Total Used FSUs) thanks to the demand balance across the links. Results show that up to 8.33 % capacity savings can be achieved on average by balanced routing.

This situation can be explained by using the shortest path concentrates the demands on several links -generally on the core section of the network- while outlying network links are under-used. The highly loaded links suffer of high fragmentation, thus increasing the overall network fragmentation. Instead, using a balanced routing technique decreases the load of the highest loaded links, which in the end diminishes the capacity required and the network fragmentation. Notwithstanding, for the ARPANET network topology, the routes obtained by both algorithms (SPR and BR) coincide on a 77.37 %, while for the remaining topologies, the percentage of coincidence is much lower. This situation explains that there is not much difference using SPR and BR on ARPANET, as previously mentioned.

These results highlight the impact of routing strategies on the network performance of static SDM-EON networks. Remark that the standard decision found in the literature to route the demands is to simply use the shortest path [13], [16], [32], [33], without applying any load balancing process. However, as we could see in Figure 4, the shortest path criteria is not the best choice in terms of effective capacity required to accommodate the network demands.

Next, we will report on simulation results evaluating the impact of the topology and the demand-sorting strategies using the BR routing.

TABLE 5. All network topologies parameters used in this work.

Topology	$\mathcal{N}$	$\mathcal{E}$	$\mathcal{U}$	$\bar{\mathcal{L}}$	$\bar{\mathcal{R}}$	$\bar{\mathcal{H}}$	$\frac{\mathcal{U}}{\mathcal{E}}$
Eurocore	11	50	110	425.6	686.76	1.58	2.2
NSFNet	14	42	82	1086.6	2530.33	2.14	4.3
ARPANet	20	62	380	609.4	1850.73	2.8	6.12
UKNet	21	78	420	138.2	369.53	2.5	5.38
EONet	20	78	380	724.3	1760.12	2.3	4.8
USNet	46	152	2070	435.5	1940.2	4.39	13.6

B. IMPACT OF THE NETWORK TOPOLOGY

Figure 5 shows the values of the Total Used FSUs (%) metric for the 34 demands sorting strategies analyzed in this paper for the Eurocore, NSFNet, EONet, UKNet, USNet and ARPANet network topologies.

It can be seen that sorting the network demands previous to the spectrum assignment significantly impacts the Total Used FSUs obtained by the RMLSSA strategies for SDM-EON architectures, irrespective of the network topology analyzed.

The worst-performing topology is the ARPANet network, where the demand sorting strategies with the worst performance achieve a Total Used FSUs (%) equal to 43.48 %. The best performing strategy, **24**-Link ↓ Distance ↑, achieves an increase of 86.22 % in Total Used FSUs (%) with respect to the worst one.

On the other hand, the best-performing topology is the Eurocore network, obtaining a Total Used FSUs (%) value equal to 72.21 % on the worst sorting strategy and equal to 93.06 % for the best strategy.

Broadly speaking, we can recognize that there are some groups of networks performing similarly. On the first group,

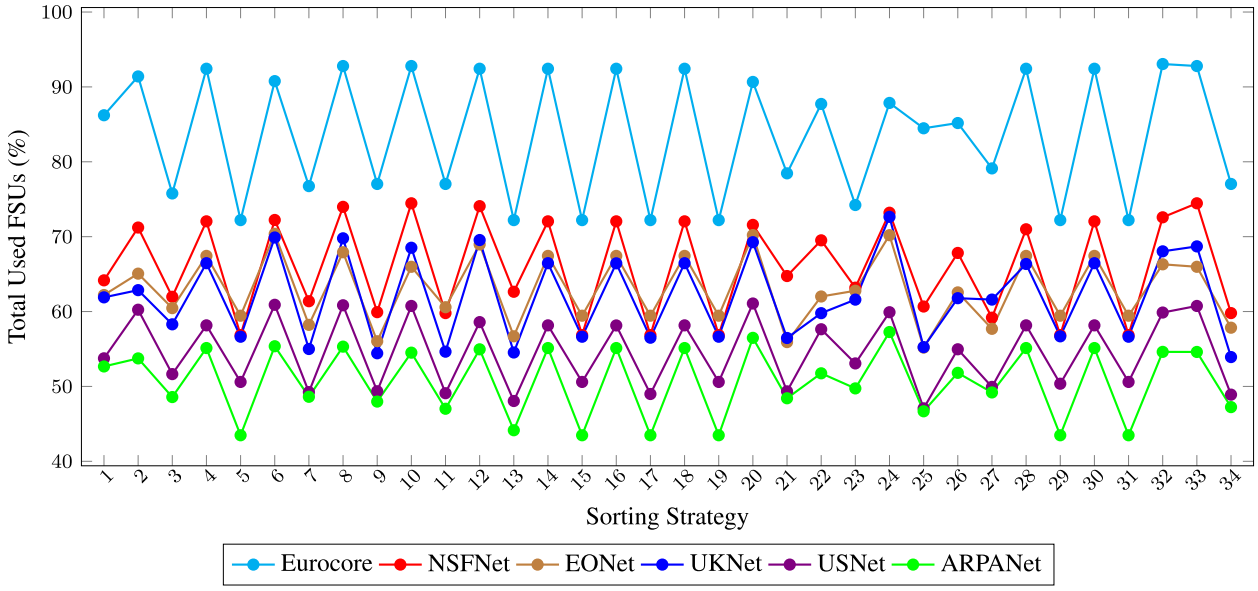

FIGURE 5. Total Used FSUs (%) obtained by the RMLSSA method using Baroni (BR) routing method and the 34 demand sorting strategies for Eurocore, NSFNet, EONet, UKNet, USNet and ARPANet network topologies.

Eurocore appears in the higher part of the figure (with a Total Used FSUs (%) performance ranging from 70 % to 90 %); secondly, the NSFNet, EONet and UKNet topologies appear in the middle zone (around 60 % to 70 % of total used FSUs); and lastly, USNet and ARPANet appear on the lower part of the figure (with Total Used FSUs (%) values between 45 % to 60 %).

Table 5 summarizes the parameters of all networks considered in this work. These parameters are the number of network nodes $\mathcal{N}$, links $\mathcal{E}$ and demands $\mathcal{U}$, the mean length of the network links $\bar{\mathcal{L}}$, the average length of routes $\bar{\mathcal{R}}$, the mean value of the number of hops per route $\bar{\mathcal{H}}$, and the ratio between the number of demands and the number of networks links $\frac{\mathcal{U}}{\mathcal{E}}$. From Table 5 and Figure 5 we can conclude that the network percentage of Total Used FSUs is inversely proportional to the size of networks (in terms of average link distances), as well as the number of connection demands using each network link.

However, the ARPANet network topology does not follow this rule, due to the fact that it is a highly symmetrical network attending many demands per link (an average of 6.12 demands per link), and the links are also very long, as shown in Table 5. The above means that most demands to be assigned require a high number of FSUs and thus, very few demands requiring a low number of FSUs which allow occupying the fragmented FSUs. As a result, ARPANet exhibits the lowest percentage of Total Used FSUs (%), despite not being the one with the largest number of nodes, links or demands.

C. IMPACT OF THE DEMAND-SORTING STRATEGIES

Finally, here we evaluate the impact of the demand sorting strategies included in the RMLSSA algorithm on the network performance.

We found out that the best strategies, in terms of effective network capacity and fragmentation, generally are the Strategies **24**-Link ↓ Distance ↑, **20**-Link ↓ FSU ↑ and **6**-Link ↓, which sort the demands using the number of links/hops on the connection paths as a primary (or only) sorting criterion in decreasing order. This conclusion differs from the standard choice found in the literature, where demands are sorted in decreased order of bandwidth requirements (number of FSUs) (Strategy **2**: FSU ↓). This situation can be explained by the impact of physical-layer impairments on the modulation format selection: Physical layer impairment considerations restrain the modulation formats to be used, to the ones with a feasible optical reach. Therefore, demands with long routes require a larger amount of FSUs than shorter path demands. Besides, routes with a greater number of links request a larger amount of resources along their paths, being the more troublesome ones from the spectrum assignment point of view (adding the bandwidth and length correlation). Then, they should be the first ones to be allocated.

To zoom in the performance of the different criteria to sort connection requests, Figures 6, 7, 8 and 9 show the percentage of FSUs used on each core for the ARPANet, UKNet, EONet and USNet network topologies, respectively. Each bar shows the distribution of the modulation formats used across the different cores together with the spectral and spatial fragmentation, while the red line represents the number of demands allocated on each core. In Figures 6, 7 and 8, the sub-figures (a) and (b) present the best sorting strategies in terms of the lowest effective capacity, lowest total fragmentation and number of cores used, and (c) shows the worst strategy for each topology. On the other hand, in Figure 9 the best sorting strategies are presented in (a) and (b) sub-figures, meanwhile (c) and (d) sub-figure illustrate the worst-case ones.

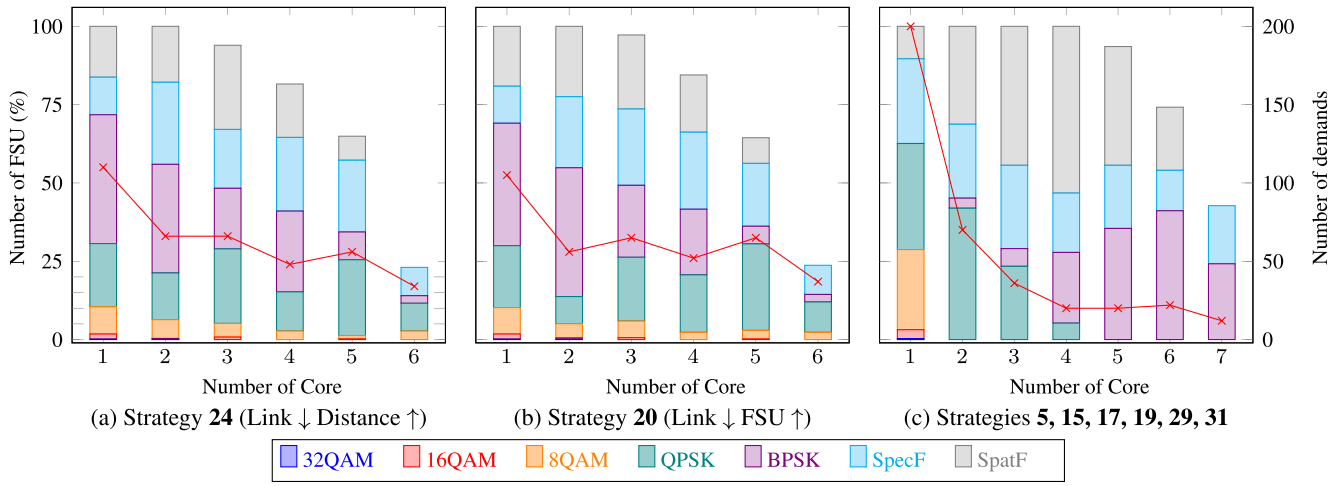

FIGURE 6. Percentage of FSUs used and number of demands in ARPANet network, taking the effective capacity as the total on each core in terms of the modulation format used and the spatial and spectral fragmentation, for the best (a) and (b), the worst (c) sorting strategies.

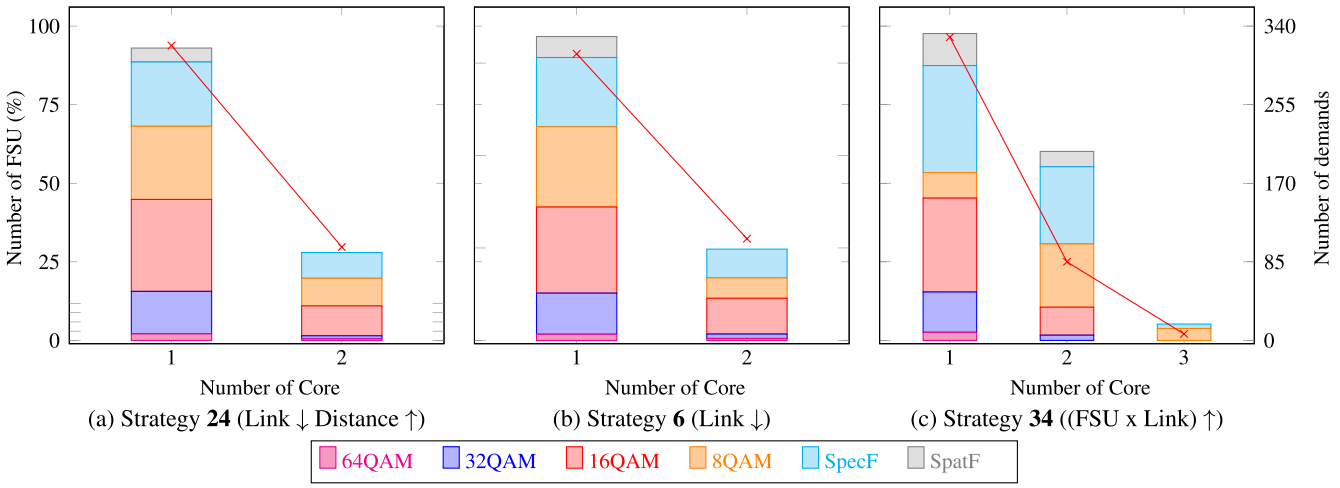

FIGURE 7. Percentage of FSUs used and number of demands in UKNet network, taking the effective capacity as the total on each core in terms of the modulation format used and the spatial and spectral fragmentation, for the best (a) and (b), the worst (c) sorting strategies.

In Figures 6, 7, 8 and 9 we can see that the best strategies allocate first the connections with the least efficient modulation formats (BPSK and QPSK), distributing them among the first network cores. The highly efficient ones (32QAM and 16QAM) are then used to fill the gaps on the network cores decreasing the fragmentation on the link cores. On the other hand, bad sorting strategies allocate first the demands using 32QAM, 16QAM and 8QAM, while leaving the other ones to be allocated on the next cores. Remark that the spectrum assignment process is First-Fit, therefore attending the demands first on the first core, and then searching sequentially among the next link cores.

In addition, Figures 6 to 9 present similarities in terms of the distribution of demands over the link cores. Generally speaking, the number of demands per core for the best sorting strategies is more uniformly distributed. In contrast, the worst-performance prioritization strategies concentrate most of the demands on the first link cores. This behavior is highlighted in Figures 6 and 9 (ARPANet and USNet respectively), because these are topologies using a large number of cores, evidencing the difference in the number of demands between the worst and best sorting strategies.

1) MIXED CRITERIA

Groups 3 and 4 in Table 2 present mixed-criteria for sorting the network demands. To the best of our understanding they are not found in the literature. Consequently, we will discuss the impact of using a second criterion to break the ties while sorting the connection demands.

As mentioned in Section I, several papers sort the connection requests according to their bandwidth demands (number of FSUs) or their path lengths (number of links on its path).

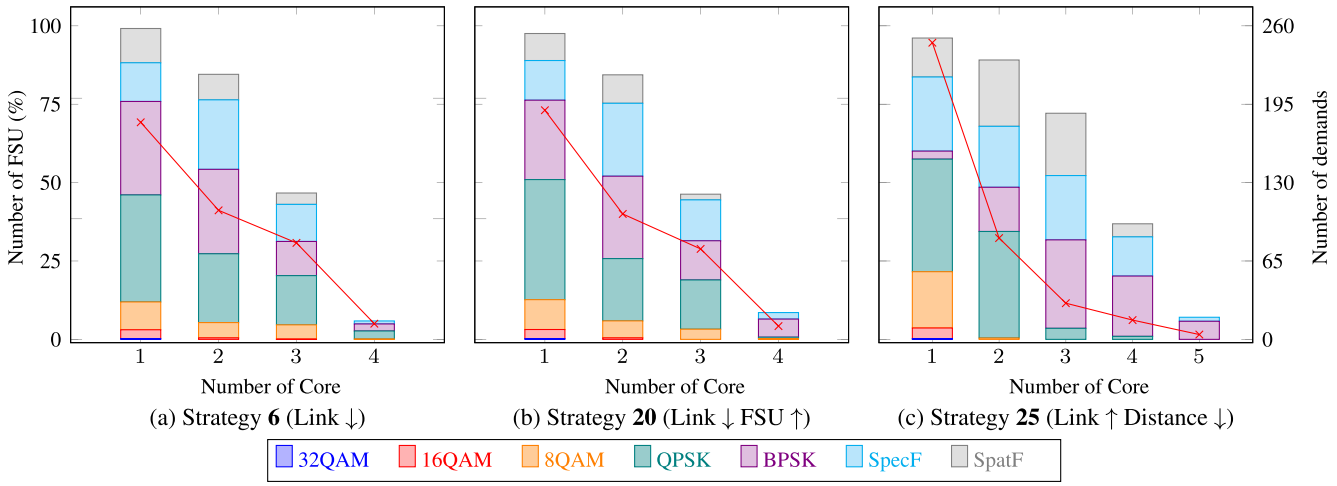

FIGURE 8. Percentage of FSUs used and number of demands in EONet network, taking the effective capacity as the total on each core in terms of the modulation format used and the spatial and spectral fragmentation, for the best (a) and (b), the worst (c) sorting strategies.

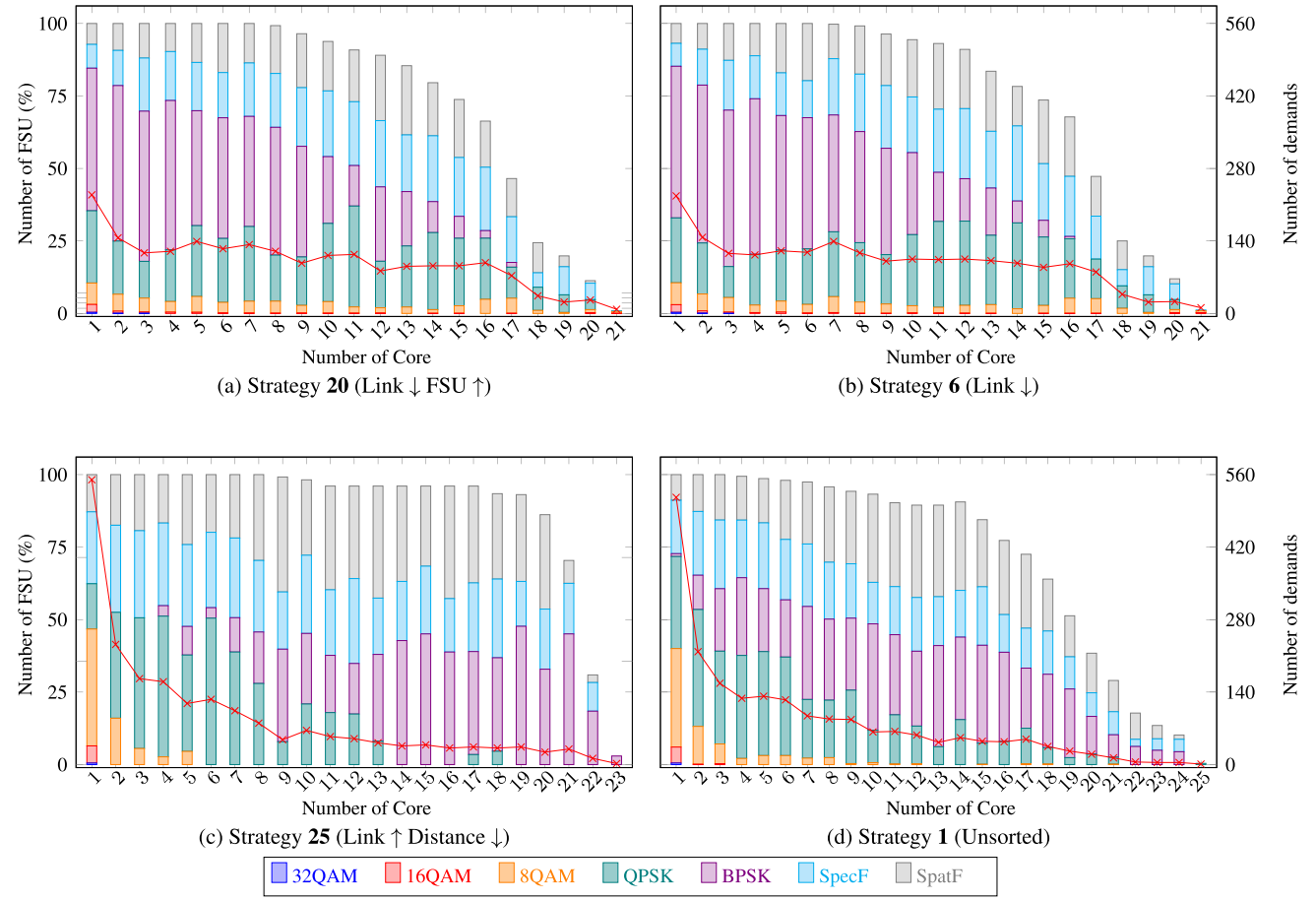

FIGURE 9. Percentage of FSUs used and number of demands in USNet network, taking the effective capacity as the total on each core in terms of the modulation format used and the spatial and spectral fragmentation, for the best (a), and the worst (b) sorting strategies.

However, our simulation results show, in general, that the order strategies with the best results in terms of network capacity (i.e. effective network capacity and the number of cores required) are strategies **24**-Link ↓ Distance ↑, **20**-Link ↓ FSU ↑ and **6**- Link ↓, prevailing strategy **24** in ARPANet and UKNet.

From the above, it is necessary to highlight how the strategies with double order criteria (**20**-Link ↓ FSU ↑ and **24**-Link ↓ Distance ↑) obtain better results in most of the topologies than strategies with a single order criterion.

The use of mixed (or double) criteria, leads to basically sorting the demands according to a first sorting criterion, and then breaking the ties obtained by the first arrangement using a second criterion. At first glance, the impact might seem scarce, or even meager. However, we measure the impact of the use of a second criterion, presenting an extra 1.33 % total used FSUs on strategies using Link ↓ as a first sorting decision between the worst-case and best-case ones, averaging the results of the 6 topologies. Similar results can be obtained on several mixed criteria comparisons. Therefore, a good decision on the second criteria, also impacts the network performance. Even more, neglecting to sort the ties obtained by the first sorting criteria may result in extra capacity (even extra cores in extreme cases).

2) SPECIAL CRITERIA

Groups 5 and 6 in Table 2 present special criteria for sorting the network demands. Again, to the best of our understanding, Group 5 is not found in the literature; and Group 6 is used in [17]. Consequently, we will discuss their impact on network performance.

In strategy **32**- + Link ↓ (FSU × Link) ↓, the demands that are in the most loaded links of the network will be assigned first, in order to reduce fragmentation in these links, since they are the most used. This strategy exhibits the highest value of Total Used FSU(%) (93.06 %) in the Eurocore network topology.

On the other hand, strategy **33**- (FSU × Link) ↓, sorts by the bandwidth demanded to the network, being one of the best strategies in the NSFNet network topology, with a total fragmentation percentage of 25.54. In this way, the importance of these special criteria is highlighted.

In general, when comparing the value of Total Used FSU (%) of the best strategies (71.48 % on average) with the worst strategies (54.79 % on average) in the 6 topologies discussed, it can be seen that up to a 16.69 % capacity savings can be achieved using the best performing demand-prioritization strategy compared to the worst-performing ones, thus emphasizing the importance of order strategies in the static SDM-EON scenarios. In addition, note that selecting an incorrect demand sorting strategy can result in an excess of cores being needed, which can translate into increased installation costs.

3) LOWER BOUNDS

Conversely, we define an ideal setting where continuity and contiguity constraints are not in place, therefore providing an effective capacity lower bound. This optimal value allows us to quantify the quality of the best performing heuristics previously analyzed. Then, we evaluate the quality of the results obtained by applying the best combination of routing and demand prioritization for each analyzed topology, computing the proximity of these strategies to the lower bound. In the Eurocore network topology, the best performing heuristic needs 6.94 % more capacity than the lower bound setting. Similarly, for the NSFNet, ARPANet, UKNet, EONet and USNet, the extra capacity needed compared to the lower bound were 7.64 %, 18.44 %, 3.65 %, 9.6 % and 17.8 %, respectively. These values show a very good performance for Eurocore, NSFnet, UKNet and EONet and acceptable performance in the ARPANet and USNet topologies.

4) FURTHER DISCUSSION

We have discussed how demand sorting strategies impact the network in terms of required capacity and network fragmentation. We note that, in general, the worst sorting strategies serve a large number of demands in a small number of cores showing more fragmentation on the remaining cores and demanding more capacity. On the other hand, best sorting strategies distribute demands across the fiber more evenly, presenting a balanced amount of connections per core and requiring less capacity in terms of FSU and the total amount of cores.

The spatial distribution of the connections may impact the network in several ways. Among them, the required node equipment and the quality of the transmitted signals. The concentration of connections in the first cores increases the PLI affecting them due to nonlinear effects. Additionally, the crosstalk arising from the heavily loaded cores can detrimentally impact neighboring cores. Moreover, if a strategy requires a greater capacity (number of cores), the fiber will present higher levels of inter-core crosstalk due to the reduced core pitch needed to accommodate them in a single cladding. Higher crosstalk levels can further reduce the MAR for all modulation formats, potentially leading to even greater capacity requirements after the RMLSSA procedure. This only highlights the importance of using good demand-prioritization strategies.

Note that, the results of this work - order strategies with better performance - can be considered as an initial solution for the design of meta-heuristic algorithms.

V. CONCLUSION

In this work, we analyzed the impact of sorting network demands, previous to the SSA step in the RMLSSA algorithm, on the network performance for static SDM-EON architectures. Besides, we examined the routing algorithm's impact, concluding that balancing the demands across the network links improves network performance.

We evaluated the performance of commonly used techniques to solve the RMLSSA algorithm, using 34 different sorting strategies. Generally speaking, the best-achieving approaches in terms of effective capacity and number of cores required are strategies **6** (Link ↓), **20** (Link ↓ FSU ↑) and **24** (Link ↓ Distance ↑), all of them ordering demands in terms of the number of hops of their paths.

As a common feature, we find that sorting criteria on a descending order tends to perform better in terms of frag-

mentation and spectrum usage, than arranging demands in ascending order. Accordingly, a good practice applies the first criteria in descending order when using mixed sorting criteria. Finally, sorting demands according to the number of links (routes with a longer number of links first) appears as the best option, as it allows attending first demands with significant resource demands to then allocate shorter route demands to fill the gaps left by the most demanding connection requests. This strategy is not common in the literature.

As seen in the simulation results, the order in which demands are allocated impacts the network resources needed significantly, affecting the percentage of used FSUs: a good selection of order strategy can increase the Total Used FSUs up to 71.48 % on average. Therefore, choosing proper criteria is critical for efficient usage of the frequency spectrum and fiber cores.

Also, the capacity requirements of the best routing algorithm (BR) and the best order strategy for each topology were compared against a lower bound. This comparison shows a very good performance of the best demand-prioritization strategies demanding from 3.65 % to 18.44 % extra network capacity than the ideal setting in the analyzed topologies.

Finally, knowing which strategy to use in a given topology offers the added value of knowing how the strategy behaves in terms of modulation formats, number of demands per core, percentage of fragmentation, percentage of Total Used FSUs, which assists network operators in the decision-making of equipment deployment.

REFERENCES

[1] M. Klinkowski, P. Lechowicz, and K. Walkowiak, "Survey of resource allocation schemes and algorithms in spectrally-spatially flexible optical networking," *Opt. Switching Netw.*, vol. 27, pp. 58–78, Jan. 2018.

[2] A. D. Ellis, N. M. Suibhne, D. Saad, and D. N. Payne, "Communication networks beyond the capacity crunch," *Phil. Trans. Roy. Soc. A, Math., Phys. Eng. Sci.*, vol. 374, no. 2062, Mar. 2016, Art. no. 20150191.

[3] O. Gerstel, M. Jinno, A. Lord, and S. J. B. Yoo, "Elastic optical networking: A new dawn for the optical layer?" *IEEE Commun. Mag.*, vol. 50, no. 2, pp. s12–s20, Feb. 2012.

[4] P. Layec, A. Morea, F. Vacondio, O. Rival, and J.-C. Antona, "Elastic optical networks: The global evolution to software configurable optical networks," *Bell Labs Tech. J.*, vol. 18, no. 3, pp. 133–151, Dec. 2013.

[5] B. Chatterjee and E. Oki, *Elastic Optical Networks: Fundamentals, Design, Control, and Management*. Boca Raton, FL, USA: CRC Press, 2020.

[6] *Spectral Grids for WDM Applications: DWDM Frequency Grid*, document ITU-T G.694.1, Telecommunication Standardization Sector of ITU, Ginebra, Switzerland, 2012.

[7] N. Sambo, A. Ferrari, A. Napoli, N. Costa, J. Pedro, B. Sommerkohrn-Krombholz, P. Castoldi, and V. Curri, "Provisioning in multi-band optical networks: A C+L+S-band use case," in *Proc. 45th Eur. Conf. Opt. Commun. (ECOC)*, 2019, pp. 1–4.

[8] A. Ferrari, E. Virgillito, and V. Curri, "Band-division vs. space-division multiplexing: A network performance statistical assessment," *J. Lightw. Technol.*, vol. 38, no. 5, pp. 1041–1049, Mar. 1, 2020.

[9] G. Li, N. Bai, N. Zhao, and C. Xia, "Space-division multiplexing: The next frontier in optical communication," *Adv. Opt. Photon.*, vol. 6, no. 4, pp. 413–487, 2014.

[10] G. M. Saridis, D. Alexandropoulos, G. Zervas, and D. Simeonidou, "Survey and evaluation of space division multiplexing: From technologies to optical networks," *IEEE Commun. Surveys Tuts.*, vol. 17, no. 4, pp. 2136–2156, Aug. 2015.

[11] E. Agrell, M. Karlsson, A. Chraplyvy, D. Richardson, P. Krummrich, P. Winzer, K. Roberts, J. Fischer, S. Savory, B. Eggleton, M. Secondini, F. R. Kschischang, A. Lord, J. Prat, I. Tomkos, J. E. Bowers, S. Srinivasan, M. Brandt-Pearce, and N. Gisin, "Roadmap of optical communications," *J. Opt.*, vol. 18, no. 6, 2016, Art. no. 063002.

[12] Ì. Brasileiro, L. Costa, and A. Drummond, "A survey on challenges of spatial division multiplexing enabled elastic optical networks," *Opt. Switching Netw.*, vol. 38, Sep. 2020, Art. no. 100584.

[13] M. Yaghubi-Namaad, A. G. Rahbar, and B. Alizadeh, "Adaptive modulation and flexible resource allocation in space-division-multiplexed elastic optical networks," *J. Opt. Commun. Netw.*, vol. 10, pp. 240–251, Mar. 2018.

[14] N. Yoshikane and T. Tsuritani, "Recent progress in space-division multiplexing optical network technology," in *Proc. Int. Conf. Opt. Netw. Design Modeling (ONDM)*, May 2020, pp. 1–4.

[15] F. Ferreira, E. Sillekens, R. Killey, and P. Bayvel, "Challenges in modelling optical fibres for spatial division multiplexing," in *Proc. IEEE Photon. Soc. Summer Top. Meeting Ser. (SUM)*, Jul. 2020, pp. 1–2.

[16] J. Perelló, J. M. Gené, J. A. Lazaro, A. Pagès, and S. Spadaro, "Assessment of flex-grid/SDM backbone networks under inter-core XT-limited transmission reach," in *Proc. Int. Conf. Photon. Switching (PS)*, Sep. 2015, pp. 190–192.

[17] A. Muhammad, G. Zervas, and R. Forchheimer, "Resource allocation for space-division multiplexing: Optical white box versus optical black box networking," *J. Lightw. Technol.*, vol. 33, no. 23, pp. 4928–4941, Dec. 1, 2015.

[18] J. Perelló, J. M. Gené, A. Pagès, J. A. Lazaro, and S. Spadaro, "Flex-grid/SDM backbone network design with inter-core XT-limited transmission reach," *IEEE/OSA J. Opt. Commun. Netw.*, vol. 8, no. 8, pp. 540–552, Aug. 2016.

[19] A. Muhammad, M. Furdek, G. Zervas, and L. Wosinska, "Filterless networks based on optical white boxes and sdm," in *Proc. 42nd Eur. Conf. Opt. Commun. (ECOC)*, 2016, pp. 1–3.

[20] F. I. Calderón, A. Lozada, D. Bórquez-Paredes, R. Olivares, E. J. Davalos, G. Saavedra, N. Jara, and A. Leiva, "BER-adaptive RMLSA algorithm for wide-area flexible optical networks," *IEEE Access*, vol. 8, pp. 128018–128031, 2020.

[21] P. Yuan and A. Xu, "The influence of physical network topologies on wavelength requirements in optical networks," *J. Lightw. Technol.*, vol. 28, no. 9, pp. 1338–1343, May 1, 2010.

[22] T. Fischer, K. Bauer, P. Merz, and K. Bauer, "Solving the routing and wavelength assignment problem with a multilevel distributed memetic algorithm," *Memetic Comput.*, vol. 1, no. 2, pp. 101–123, Jun. 2009.

[23] A. Zapata-Beghelli and P. Bayvel, "Dynamic versus static wavelength-routed optical networks," *J. Lightw. Technol.*, vol. 26, no. 20, pp. 3403–3415, Oct. 15, 2008.

[24] M. Ruiz, L. Velasco, A. Lord, D. Fonseca, M. Pioro, R. Wessaly, and J. Fernandez-Palacios, "Planning fixed to flexgrid gradual migration: Drivers and open issues," *IEEE Commun. Mag.*, vol. 52, no. 1, pp. 70–76, Jan. 2014.

[25] P. Lechowicz, R. Goscien, R. Rumipamba-Zambrano, J. Perello, S. Spadaro, and K. Walkowiak, "Greenfield gradual migration planning toward spectrally-spatially flexible optical networks," *IEEE Commun. Mag.*, vol. 57, no. 10, pp. 14–19, Oct. 2019.

[26] N. Jara, J. Salazar, and R. Vallejos, "A spiral approach to solve the routing and spectrum assignment problem in ring topologies for elastic optical networks," in *Proc. 9th Int. Conf. Simulation Modeling Methodol., Technol. Appl.*, 2019, pp. 269–276.

[27] J. Yuan, R. Zhu, Y. Zhao, Q. Zhang, X. Li, D. Zhang, and A. Samuel, "A spectrum assignment algorithm in elastic optical network with minimum sum of weighted resource reductions in all associated paths," *J. Lightw. Technol.*, vol. 37, no. 21, pp. 5583–5592, Nov. 1, 2019.

[28] F. S. Abkenar and A. G. Rahbar, "Study and analysis of routing and spectrum allocation (RSA) and routing, modulation and spectrum allocation (RMSA) algorithms in elastic optical networks (EONs)," *Opt. Switching Netw.*, vol. 23, pp. 5–39, Jan. 2017.

[29] S. Talebi, F. Alam, I. Katib, M. Khamis, R. Salama, and G. N. Rouskas, "Spectrum management techniques for elastic optical networks: A survey," *Opt. Switching Netw.*, vol. 13, pp. 34–48, Jul. 2014.

[30] N. Jara, J. Salazar, and R. Vallejos, "A topology-based spectrum assignment solution for static elastic optical networks with ring topologies," *IEEE Access*, vol. 8, pp. 218828–218837, 2020.

[31] V. López and L. Velasco, *Elastic Optical Networks: Architectures, Technologies, and Control*. Cham, Switzerland: Springer, 2016.

[32] A. Muhammad, G. Zervas, D. Simeonidou, and R. Forchheimer, "Routing, spectrum and core allocation in flexgrid SDM networks with multi-core fibers," in *Proc. Int. Conf. Opt. Netw. Design Modeling*, 2014, pp. 192–197.

[33] H. Wu, F. Zhou, Z. Zhu, and Y. Chen, "Analysis framework of RSA algorithms in elastic optical rings," *J. Lightw. Technol.*, vol. 37, no. 4, pp. 1113–1122, Feb. 15, 2019.

[34] K. Christodoulopoulos, I. Tomkos, and E. A. Varvarigos, "Elastic bandwidth allocation in flexible OFDM-based optical networks," *J. Lightw. Technol.*, vol. 29, no. 9, pp. 1354–1366, May 1, 2011.

[35] K. Christodoulopoulos, I. Tomkos, and E. A. Varvarigos, "Routing and spectrum allocation in OFDM-based optical networks with elastic bandwidth allocation," in *Proc. IEEE Global Telecommun. Conf. (GLOBECOM)*, Dec. 2010, pp. 1–6.

[36] B. Shariati, P. S. Khodashenas, J. M. Rivas-Moscoso, S. Ben-Ezra, D. Klonidis, F. Jiménez, L. Velasco, and I. Tomkos, "Evaluation of the impact of different SDM switching strategies in a network planning scenario," in *Proc. Opt. Fiber Commun. Conf.*, 2016, pp. 1–3, Paper Tu2H-4.

[37] B. Shariati, D. Klonidis, J. M. Rivas-Moscoso, and I. Tomkos, "Evaluation of the impact of spatial and spectral granularities on the performance of spatial superchannel switching schemes," in *Proc. 18th Int. Conf. Transparent Opt. Netw. (ICTON)*, Jul. 2016, pp. 1–4.

[38] H. Xuan, Y. Wang, S. Hao, Z. Xu, X. Li, and X. Gao, "Security-aware routing and core allocation in elastic optical network with multi-core," in *Proc. 12th Int. Conf. Comput. Intell. Secur. (CIS)*, Dec. 2016, pp. 294–298.

[39] J. Rivas-Moscoso, B. Shariati, A. Mastropaolo, D. Klonidis, and I. Tomkos, "Cost benefit quantification of sdm network implementations based on spatially integrated network elements," in *Proc. 42nd Eur. Conf. Opt. Commun. (ECOC)*, 2016, pp. 1–3.

[40] L. Zhang, N. Ansari, and A. Khreishah, "Anycast planning in space division multiplexing elastic optical networks with multi-core fibers," *IEEE Commun. Lett.*, vol. 20, no. 10, pp. 1983–1986, Oct. 2016.

[41] M. N. Dharmaweera, L. Yan, M. Karlsson, and E. Agrell, "Nonlinear-impairments- and crosstalk-aware resource allocation schemes for multicore-fiber-based flexgrid networks," in *Proc. 42nd Eur. Conf. Opt. Commun. (ECOC)*, 2016, pp. 1–3.

[42] Y. Zhao, Y. Zhu, C. Wang, X. Yu, C. Liu, B. Li, and J. Zhang, "Superchannel oriented routing, spectrum and core assignment under crosstalk limit in spatial division multiplexing elastic optical networks," *Opt. Fiber Technol.*, vol. 36, pp. 249–254, Jul. 2017.

[43] Y. Zhou, Q. Sun, and S. Lin, "Link state aware dynamic routing and spectrum allocation strategy in elastic optical networks," *IEEE Access*, vol. 8, pp. 45071–45083, 2020.

[44] K. Walkowiak, M. Klinkowski, B. Rabiega, and R. Goścień, "Routing and spectrum allocation algorithms for elastic optical networks with dedicated path protection," *Opt. Switching Netw.*, vol. 13, pp. 63–75, Jul. 2014.

[45] J. Zhao, H. Wymeersch, and E. Agrell, "Nonlinear impairment-aware static resource allocation in elastic optical networks," *J. Lightw. Technol.*, vol. 33, no. 22, pp. 4554–4564, Nov. 15, 2015.

[46] R. Rumipamba-Zambrano, J. Perello, and S. Spadaro, "Route, modulation format, MIMO, and spectrum assignment in flex-grid/MCF transparent optical core networks," *J. Lightw. Technol.*, vol. 36, no. 16, pp. 3534–3546, Aug. 15, 2018.

[47] Y. Zhao, L. Hu, R. Zhu, X. Yu, X. Wang, and J. Zhang, "Crosstalk-aware spectrum defragmentation based on spectrum compactness in space division multiplexing enabled elastic optical networks with multicore fiber," *IEEE Access*, vol. 6, pp. 15346–15355, Jan. 2018.

[48] S. K. Singh and A. Jukan, "Efficient spectrum defragmentation with holding-time awareness in elastic optical networks," *J. Opt. Commun. Netw.*, vol. 9, no. 3, p. B78, Mar. 2017.

[49] E. J. Dávalos, M. F. Romero, S. M. Galeano, D. A. Báez, A. Leiva, and B. Baran, "Spectrum defragmentation in elastic optical networks: Two approaches with metaheuristics," *IEEE Access*, vol. 7, pp. 119835–119843, 2019.

[50] A. N. Patel, P. N. Ji, J. P. Jue, and T. Wang, "Defragmentation of transparent flexible optical WDM (FWDM) networks," in *Proc. Opt. Fiber Commun. Conf./Nat. Fiber Opt. Eng. Conf.*, 2011, pp. 1–3.

[51] X. Chen, A. Jukan, and A. Gumaste, "Multipath de-fragmentation: Achieving better spectral efficiency in elastic optical path networks," in *Proc. IEEE INFOCOM*, Apr. 2013, pp. 390–394.

[52] P. Poggiolini, G. Bosco, A. Carena, V. Curri, Y. Jiang, and F. Forghieri, "The GN-model of fiber non-linear propagation and its applications," *J. Lightw. Technol.*, vol. 32, no. 4, pp. 694–721, Feb. 15, 2014.

[53] J. Y. Yen, "Finding the K shortest loopless paths in a network," *Manage. Sci.*, vol. 17, pp. 712–716, Jul. 1971.

[54] E. W. Dijkstra, "A note on two problems in connexion with graphs," *Numerische Math.*, vol. 1, no. 1, pp. 269–271, Dec. 1959.

[55] N. Jara, R. Vallejos, and G. Rubino, "A method for joint routing, wavelength dimensioning and fault tolerance for any set of simultaneous failures on dynamic WDM optical networks," *Opt. Fiber Technol.*, vol. 38, pp. 30–40, Nov. 2017.

[56] R. T. Koganti and D. Sidhu, "Analysis of routing and wavelength assignment in large WDM networks," *Procedia Comput. Sci.*, vol. 34, pp. 71–78, Jan. 2014.

[57] F.-J. Moreno-Muro, R. Rumipamba-Zambrano, P. Pavón-Marino, J. Perelló, J. M. Gené, and S. Spadaro, "Evaluation of core-continuity-constrained ROADMs for flex-grid/MCF optical networks," *IEEE/OSA J. Opt. Commun. Netw.*, vol. 9, no. 11, pp. 1041–1050, Nov. 2017.

[58] J. M. Simmons, *Optical Network Design and Planning*. Boston, MA, USA: Springer, 2014.

[59] B. C. Chatterjee, S. Ba, and E. Oki, "Fragmentation problems and management approaches in elastic optical networks: A survey," *IEEE Commun. Surveys Tuts.*, vol. 20, no. 1, pp. 183–210, 1st Quart., 2018.

[60] C. Rottondi, P. Boffi, P. Martelli, and M. Tornatore, "Routing, modulation format, baud rate and spectrum allocation in optical metro rings with flexible grid and few-mode transmission," *J. Lightw. Technol.*, vol. 35, no. 1, pp. 61–70, Jan. 1, 2017.

[61] S. Baroni and P. Bayvel, "Wavelength requirements in arbitrarily connected wavelength-routed optical networks," *J. Lightw. Technol.*, vol. 15, no. 2, pp. 242–251, Feb. 1997.

PATRICIA MORALES received the bachelor's degree in telecommunications and electronics engineering from the Universidad Central Marta Abreu de Las Villas, Cuba, in 2016. She is currently pursuing the Ph.D. degree in electronic engineering with Universidad Técnica Federico Santa María, Chile.

ASTRID LOZADA received the M.Sc. degree in electronic engineering from Universidad Técnica Federico Santa María (UTFSM), Chile, in 2020, where she is currently pursuing the Ph.D. degree in electronic engineering.

DANILO BÓRQUEZ-PAREDES received the B.Eng. degree and the professional title in telematics engineering from Universidad Técnica Federico Santa María (UTFSM), Valparaiso, Chile, in 2012, and the Ph.D. degree from Universidad Adolfo Ibañez, in September 2018. He is currently a full-time Professor with the Engineering and Sciences Faculty, Universidad Adolfo Ibañez. His research interests include the dynamic allocation of resources in flexible optical networks, network virtualization, graph theory, and optimization.

RICARDO OLIVARES received the B.Sc. degree in electronic engineering from Universidad Técnica Federico Santa María (UTFSM), Chile, in 1983, and the M.Sc. and D.Sc. degrees in electrical engineering from the Pontificia Universidade Católica do Rio de Janeiro, Brazil, in 1994 and 2001, respectively. He has been with the Department of Electronic Engineering, UTFSM, since 1986, where he has been the Head of Department since 2017. His current interests include RF measurements, fiber optic communication systems, fiber optical sensors, and nonlinear fiber optics.

GABRIEL SAAVEDRA (Member, IEEE) received the B.Eng. degree in telecommunication engineering and the M.Sc. degree from the Universidad de Concepción, Chile, in 2013 and 2014, respectively, and the Ph.D. degree from University College London (UCL), London, U.K., in 2019. He is currently an Associate Professor with the Universidad de Concepción. His research interests include nonlinear fiber effects, nonlinear compensation methods, and digital signal processing for optical communications.

ARIEL LEIVA (Member, IEEE) received the B.Sc. degree in electronic engineering and the M.Sc. degree in electrical engineering from Pontificia Universidad Católica de Valparaíso (PUCV), Chile, in 2003 and 2007, respectively, and the Ph.D. degree from Universidad Técnica Federico Santa María, Valparaiso, Chile, in 2013. He is currently a Lecturer with PUCV. His current research interests include fiber optic communication systems and optical networking.

ALEJANDRA BEGHELLI received the B.Eng. degree in electronic engineering and the M.Sc. degree from Universidad Técnica Federico Santa María, Chile, in 1996 and 2001, respectively, and the Ph.D. degree from University College London (UCL), London, U.K., in 2006. She is currently a Lecturer with the Department of Electronic and Electrical Engineering, UCL. Her current research interests include dynamic resource allocation in optical networks, with an emphasis on the application of artificial intelligence techniques.

NICOLÁS JARA (Member, IEEE) received the B.Sc. degree in telematics engineering and the M.Sc. degree in telematics engineering from Universidad Técnica Federico Santa María (UTFSM), Chile, in 2010, and the double Ph.D. degrees from the Université de Rennes I, France and UTFSM, in 2017 and 2018, respectively. He is currently an Assistant Professor with the Department of Electronics, UTFSM. His current research interests include optical networks design, networks performability, and simulation techniques.